Disjoining pressure and thinning transitions in smectic-*A* liquid crystal films

F. Picano, P. Oswald, and E. Kats*
Laboratoire de Physique de l'Ecole Normale Supérieure de Lyon,† 46 Allée d'Italie, 69364 Lyon Cedex 07, France
(Received 8 June 2000; published 23 January 2001)

The contact angle between a free standing film of a smectic-*A* liquid crystal and its meniscus is different from zero. It increases independently of the meniscus size when the film thickness decreases. This angle provides a very precise measurement of the film tension and of the interactions between the two free surfaces. This interaction is attractive and can be qualitatively explained within the framework of the de Gennes theory of the presmectic state. According to this model, the attraction is caused by an increase of the smectic order parameter at the free surface. This phenomenon also explains the metastability of very thin smectic films above the bulk smectic-*A*–nematic phase transition. The temperatures $T(N)$ of spontaneous thinning from N layers to $N-1$ layers is measured in the smectic phase of the liquid crystal 8CB (octylcyanobiphenyl).

DOI: 10.1103/PhysRevE.63.021705 PACS number(s): 61.30.−v, 64.70.Md, 68.03.Cd, 68.35.Md

I. INTRODUCTION

Smectic-*A* liquid crystals can form stable free standing films, similar to soap films, when they are stretched on a solid frame. Friedel [1] discovered this property in 1922 and used it as an argument in favor of the layered structure of the smectic phase in thermotropic liquid crystals. This crucial point, although quite intuitive, needs some explanations, which we give in this paper.

The interest for free smectic films was renewed in the 1970s with many beautiful works on their structure and their mechanical or thermodynamical properties. Many of the most important papers in these fields can be found in the book by Pershan [2]. All these works focused on the properties of the film itself and evade the problem of the meniscus that forms between the film and its support. In fact the meniscus acts as a reservoir with which the film can exchange matter. In this respect, the meniscus plays the important role of fixing the chemical potential (or the pressure) in the film. Pieranski was the first to draw attention to this problem [3] in 1993 but it is only recently that a theory of the meniscus has been proposed [4,5]. According to this model, two regions must be distinguished [5]: one with large density of dislocations in which focal domains and oily streaks form and another, with medium density of dislocations, where dislocations remain elementary [5], i.e., of Burgers vector $b=d$ where d is the layer thickness. The former corresponds to the thick parts of the meniscus whereas the latter is next to the film and has a circular profile of radius of curvature R. In thick films (more than 50 layers), the circular profile matches tangentially the free surface of the film while its radius of curvature fixes the pressure inside both the meniscus and the film via the Laplace law:

$$\Delta P = P_{\text{air}} - P_{\text{smectic}} = \frac{\gamma}{R} \tag{1}$$

with γ the air–smectic surface free energy. In this limit, the pressure difference across the free surface in the film is equilibrated by the compression of the smectic layers. This pressure difference also changes the film tension τ which reads

$$\tau = 2\gamma + \Delta P H, \tag{2}$$

where H is the film thickness. This dependence has been first observed experimentally by Pieranski *et al.* [3].

In this paper, we show first experimentally that in thin films, the meniscus no longer matches the film tangentially, but makes an apparent ''contact'' angle $\theta_m \neq 0$ which increases when the film thickness decreases (Sec. II). The origin of this angle and its consequences on the film tension are analyzed from a mechanical point of view in the next section: in particular, we show that this angle is associated with some disjoining pressure in the film (Sec. III). The origin of this ''extra'' pressure is discussed in the framework of the de Gennes theory for presmectic films [6,7] (Sec. IV). We then describe the successive thinning transitions of a smectic-*A* film that occur when the film is heated above T_{NA} (the bulk transition temperature to the nematic phase) (Sec. V). Finally, we discuss the role of boundary conditions and the scaling laws for the thinning transition temperatures (Sec. VI).

II. EXPERIMENTAL EVIDENCE OF A CONTACT ANGLE

The liquid crystal chosen is 8CB (4-*n*-octylcyanobiphenyl). It is smectic-*A* at room temperature and has a quasi-second-order phase transition to the nematic phase at 33.4 °C (for a discussion about the order of the transition see Ref. [8]).

The films are stretched on a circular frame (5 mm in diameter and 0.1 mm thick). The frame is placed in an oven whose temperature is controlled within 0.05 °C. The film is observed with a video camera via reflected light microscopy. Its thickness is obtained by measuring the reflectivity as a function of the light wavelength. The microscope is equipped with a monochromator and an optical chopper, and the intensity of the reflected light is measured by a photodiode con-

*Permanent address: Laue-Langevin Institute, Avenue de Martyrs, 38042, Grenoble Cedex, France.
†Associé au CNRS, UMR 5672.

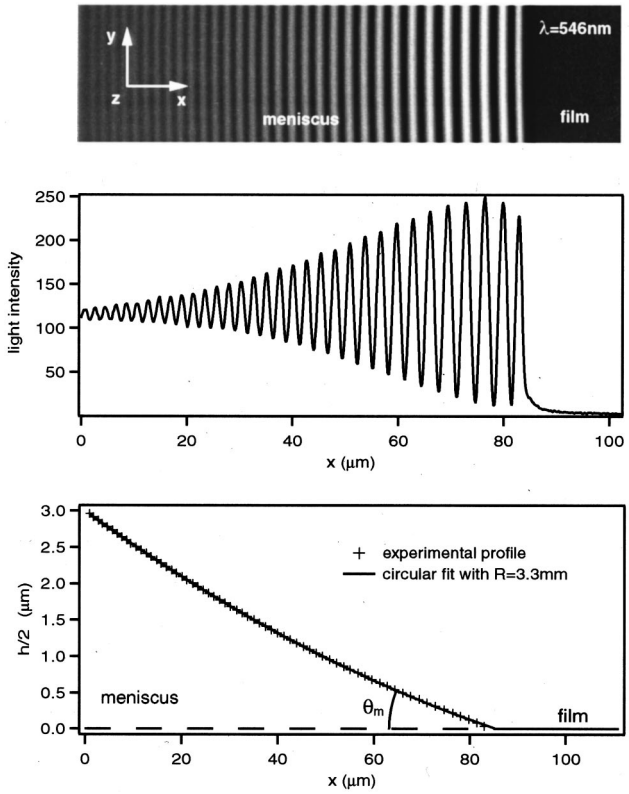

FIG. 1. (a) Fringes observed in the meniscus in monochromatic light; (b) intensity profile; (c) meniscus profile and its circular fit (solid line). Note that the contact angle θ_m is different from zero.

nected to a lock-in amplifier. In this way, the number N of layers can be exactly determined. The profile of the meniscus that forms along the sides of the frame is determined by observing in monochromatic light the fringes that form at equilibrium (note that several hours are necessary to equilibrate the film and its meniscus). More precisely, we measure the positions of the maxima and of the minima, knowing that the thickness changes of $\lambda/4n$ (n is the smectic refraction index) between a bright and a dark line. An example is given in Fig. 1. The film is six layers thick and the meniscus profile is circular [4,5] of radius of curvature $R=3.3$ mm. The new observation is that the meniscus no longer matches the film tangentially, as we have observed previously for thick films, but rather makes an apparent contact angle θ_m different from

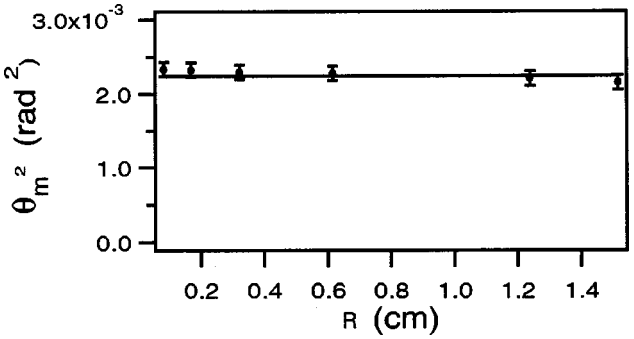

FIG. 2. Angle θ_m^2 as a function of the radius of curvature of the meniscus R ($N=6$, $T=28.7\,^\circ$C).

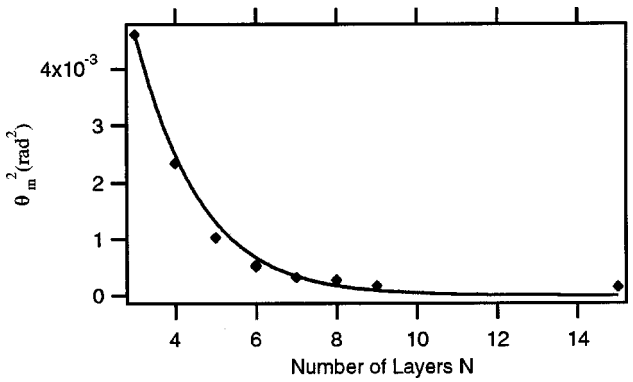

FIG. 3. Angle θ_m^2 as a function of the number of layers N in the film at $T=28.7\,^\circ$C. The solid line has been calculated from the model [Eq. (26)] by taking $\alpha_o\xi_o\psi_s^2/\gamma=7.4\times10^{-4}\,\mathrm{K}^{-1}$, $A=10k_BT$ and $\xi_o=0.8$ nm.

zero. We emphasize that θ_m is the macroscopic angle between the free surface of the film and the circle that fits the meniscus ''far'' from the intersection point (see also Fig. 5 of the next section). We performed systematic measurements of this angle as a function of radius of curvature, the film thickness and the temperature. Figure 2 shows that θ_m is independent of R, and hence of ΔP. By contrast, θ_m increases when the film thickness decreases (Fig. 3). Below T_{NA}, it also increases when the temperature increases whereas it passes through a maximum above T_{NA} (Fig. 4). We emphasize that it was possible to measure θ_m for temperatures higher than T_{NA}. This means that films can be overheated without breaking, a phenomenon that will be discussed in detail in Sec. V. In the next section, we analyze the origin of this angle and recall the concept of disjoining pressure [9].

III. MECHANICAL EQUILIBRIUM AND DISJOINING PRESSURE

Let us consider the smectic phase confined between two surfaces separated by a distance h (Fig. 5). There can occur

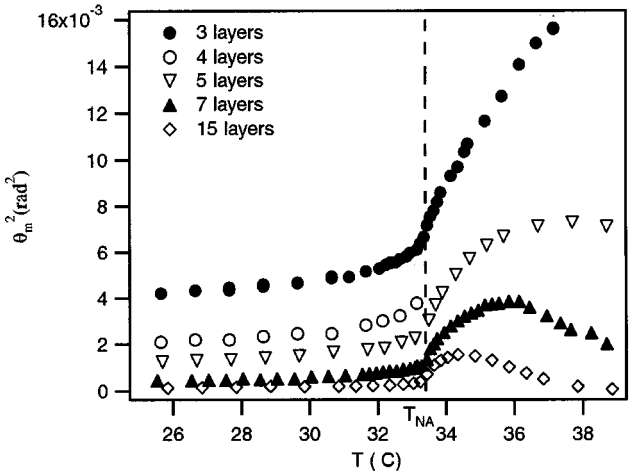

FIG. 4. Angle θ_m^2 as a function of the temperature for different values of N.

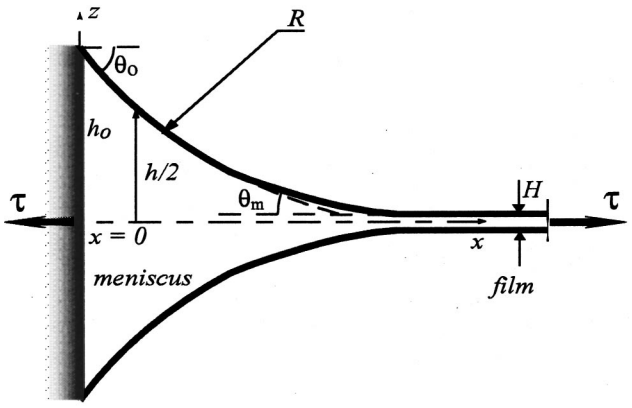

FIG. 5. Schematic representation of the film and of the meniscus. Angle θ_m is just an ''extrapolated'' macroscopic angle. Indeed, there is no angular discontinuity at small scale between the film and its meniscus. It turns out that the matching region is too small to be observable in the microscope, which gives the appearance of an angular matching.

an excess of free energy $f(h)$ (per unit surface) because of the presence of the two surfaces and of the finite thickness h of the sample. By convention, we choose $f(\infty)=0$ when the smectic is not stressed. The disjoining pressure is defined to be

$$\Pi_d=-\frac{df}{dh}. \tag{3}$$

The origin of $f(h)$ (or Π_d) is discussed in the next section. To derive the equations for mechanical equilibrium, let us first consider the total energy of the system film+meniscus. It reads [x is the axis coordinate (see Fig. 5)]:

$$F[h(x)]=\int dx\left[2\gamma\sqrt{1+\left(\frac{d(h/2)}{dx}\right)^2}+\Delta P h(x)+f[h(x)]-E[h(x)]\frac{1}{d}\frac{dh}{dx}\right]. \tag{4}$$

The first term corresponds to the surface energy and the second one to the work of the pressure (at equilibrium the pressure is the same in the film and in the meniscus) with $\Delta P=P_{\text{air}}-P_{\text{smectic}}$. The third term $f(h)$ is the excess of free energy due to the finite thickness of the system while the last one corresponds to the energy of the dislocations in the meniscus ($E[h(x)]$ is the energy of an elementary dislocation, d is the layer thickness and $-(1/d)(dh/dx)$ is the density of dislocations). Minimization with respect to h gives

$$\Delta P+\frac{df}{dh}-\gamma\frac{[d^2(h/2)/dx^2]}{[1+(d(h/2)/dx)^2]^{3/2}}=0. \tag{5}$$

This equation can be written in the equivalent form

$$\Delta P-\Pi_d-\gamma/R=0, \tag{6}$$

where Π_d is the disjoining pressure defined in (3) and R the radius of curvature at the free surface. This general equation applies both to the film and to the meniscus. Thus

$$\Delta P=\Pi_d \quad \text{in the film} \quad (R=\infty) \tag{7}$$

and

$$\Delta P=\gamma/R \quad \text{far in the meniscus where} \quad f(h)\approx 0. \tag{8}$$

Equation (7) describes the mechanical equilibrium in the film. Equation (8) is equivalent to the Laplace law for an ordinary liquid [4,5]. We emphasize that this law does strictly apply in the thick region of the meniscus.

To determine the macroscopic matching angle θ_m between the circular profile given by (8) and the film surface, we integrate Eq. (5). It gives immediately

$$\Delta P h+f[h(x)]+2\gamma\cos\theta=c, \tag{9}$$

where c is a constant of integration and θ the local angle between the free surface and the x axis [$\tan\theta=d(h/2)/dx$]. The angle θ_m measured experimentally is obtained by extrapolating at small h the circular profile given by the Laplace law (8) and by taking the corresponding value of θ at $h=H$ where H is the film thickness. This procedure gives

$$2\gamma(\cos\theta_m-1)=f(H). \tag{10}$$

Note that this equation only makes sense when $f(H)<0$ [with the convention that $f(\infty)=0$ when the smectic is not stressed]. Note also that the mechanical equilibrium $\Delta P=\Pi_d$ in the film gives $df/dh<0$ (because experimentally, $\Delta P>0$) and that the film stability requires a positive compressibility, i.e., $d^2f/dh^2>0$.

For completeness, we give the expression of the film tension τ. This is the force per unit length you must apply to maintain the film is equilibrium (Fig. 5). It is given by

$$\tau=2\gamma+\Delta P H+f(H). \tag{11}$$

This equation generalizes Eq. (2) and can be easily found by calculating the force that the meniscus exerts on the left-hand wall (Fig. 5). This calculation gives

$$\tau=2\gamma\cos\theta_o+\Delta P h_o. \tag{12}$$

Because $h_o=H+2R(\cos\theta_m-\cos\theta_o)$ and $\Delta P=\gamma/R$ [Eq. (8)] we obtain

$$\tau=\Delta P H+2\gamma\cos\theta_m \tag{13}$$

which is equivalent to Eq. (11) according to Eq. (10). Equation (13) shows that measuring θ_m is a very precise method to find the variation of the film tension caused by the interactions between the free surfaces. As θ_m is experimentally very small we can take

$$2(\cos\theta_m-1)=-\theta_m^2$$

in the following.

We discuss now the origin of $f(h)$.

IV. ORIGIN OF THE DISJOINING PRESSURE

A. Smectic-*A* elasticity

There is a first contribution to $f(h)$ that comes from the smectic elasticity only and is independent of the interactions between the two free surfaces. Indeed, the layers are stressed because the pressure in the film is less than the atmospheric pressure ($\Delta P>0$). If the film is thick enough, $f(h)$ reduces to the compression energy of the layers

$$f_e(h)=\frac{1}{2}BNd\left(\frac{h-Nd}{Nd}\right)^2, \tag{14}$$

where N is the number of layers of the film and B is the compressibility modulus of the layers below T_{NA}. In this limit, the mechanical equilibrium of the film reads

$$\Delta P=\Pi_d=-\left(\frac{df_e(h)}{dh}\right)_{h=H}=-B\frac{H-Nd}{Nd}. \tag{15}$$

In this form, the disjoining pressure is identified to $-\sigma$, where σ is the usual stress tensor [4,5] and the film tension reads

$$\tau=2\gamma+\Delta PH+f_e(H)=2\gamma+\Delta PH+\frac{\Delta P^2}{2B}H. \tag{16}$$

This formula is a generalization of Eq. (2) which takes into account the compressibility energy of the layers. Nevertheless, this term is always negligible with respect to the first correction in ΔPH because $\Delta P\ll B$ in usual experiments. Indeed $\Delta P\leqslant 2\times 10^3$ erg/cm^3 [4,5] whereas $B>10^7$ erg/cm^3, even very close to T_{NA} [10].

As a conclusion, the tension of thick films (in which interactions between free surfaces may be neglected) is given by Eq. (2) to an excellent approximation. In these films, the matching angle θ_m between the meniscus and the film must also be very close to zero [according to Eq. (10)]. This is indeed observed experimentally [4,5].

We now discuss the case of thin films ($N<20$) in which θ_m is different from 0. In this case, van der Waals interactions as well as the variations near the free surface of the amplitude of the smectic order parameter must also be taken into account.

B. Interaction between the two free surfaces

When the two free surfaces are close enough, their interaction can no longer be neglected. The most common is the van der Waals interaction that gives a power law of type

$$f_{\mathrm{vdw}}(h)=-\frac{A}{12\pi h^2}. \tag{17}$$

Constant A is known as the Hamaker constant and is typically of the order of $10k_BT$ [11]. This interaction arises from the interplay of electromagnetic field fluctuations with boundary conditions. In liquid crystals, analogous pseudo-van der Waals interactions also arise from orientational or positional fluctuations [12] but these corrections are usually small. In the following, A includes van der Waals+pseudo-van der Waals interactions.

This law gives

$$\theta_m^2=\frac{A}{12\pi\gamma h^2}. \tag{18}$$

This equation predicts that θ_m^2 decreases as $1/N^2$ at small thickness, which disagrees with our observations. Furthermore, this law cannot explain the strong dependence of θ_m on the temperature (Fig. 4) and gives too small values of θ_m^2 (with $A\approx 10k_BT$, $h=90$ Å, we calculate $\theta_m^2=5\times 10^{-4}$ rad^2, to be compared with the experimental value 4×10^{-3} rad^2). Our conclusion is that van der Waals interactions alone cannot explain our observations.

Another phenomenon that gives an attractive interaction is the increase of the amplitude of the smectic order parameter at the free surfaces. Such an increase occurs when the molecules prefer a homeotropic orientation at the free surface, which is usually observed experimentally. This model, which is a generalization of the de Gennes model for presmectic films above T_{NA} [6,7], has already been used successfully by Richetti *et al.* [13] for explaining the attractive background that is observed at small distances in a force machine with a lyotropic lamellar phase.

Let Ψ be the amplitude of the order parameter in the smectic-*A* phase and ϕ its phase (which is related to the layer displacement u by the relation $\phi=2\pi u/d$). The bulk Landau energy per unit volume reads [14]

$$f_L=\tfrac{1}{2}\alpha\Psi^2+\tfrac{1}{4}\beta\Psi^4+\cdots \tag{19}$$

with $\alpha=\alpha_o(T-T_{NA})$. Parameters α_o and β are two positive constants.

In an infinite medium, the order parameter that minimizes (19) is equal to

$$\Psi_b=\sqrt{\frac{-\alpha}{\beta}}. \tag{20}$$

In a film of thickness h, the order parameter shifts a little from its value Ψ_b because of the presence of the two free surfaces. In this case, a term in $|\mathrm{grad}(\Psi e^{i\phi})|^2$ must also be introduced to describe the spatial variation of the order parameter. Setting $\psi=\Psi-\Psi_b$, it gives within a constant:

$$f(h)=\int_{-h/2}^{h/2}\left[-\alpha\psi^2+\cdots+\frac{1}{2}L\left(\frac{d\psi}{dz}\right)^2+\frac{1}{2}L\Psi^2\left(\frac{d\phi}{dz}\right)^2\right]dz. \tag{21a}$$

For simplicity, we shall assume in the following that ψ is very small and we will replace Ψ^2 by Ψ_b^2 in the previous equation. In this limit, the energy becomes

$$f(h)=\int_{-h/2}^{h/2}\left[-\alpha\psi^2+\cdots+\frac{1}{2}L\left(\frac{d\psi}{dz}\right)^2+\frac{1}{2}L\Psi_b^2\left(\frac{d\phi}{dz}\right)^2\right]dz \tag{21b}$$

or, equivalently, by introducing the layer displacement and the bulk elastic modulus $B=4\pi^2 L\Psi_b^2/d^2$ (supposed thickness invariant):

$$f(h)=\int_{-h/2}^{h/2}\left[-\alpha\psi^2+\cdots+\frac{1}{2}L\left(\frac{d\psi}{dz}\right)^2+\frac{1}{2}B\left(\frac{du}{dz}\right)^2\right]dz. \tag{21c}$$

This assumption greatly simplifies the problem because ψ and ϕ (or u) are now completely uncoupled.

Minimization of (21c) with respect to ψ gives the differential equation

$$\xi^2\frac{d^2\psi}{dz^2}=2\psi \tag{22}$$

to which we add boundary conditions

$$\psi(-h/2)=\psi(h/2)=\psi_s, \tag{23}$$

where the excess of smectic order parameter ψ_s at the free surfaces is assumed to be constant. We define the correlation length $\xi=\sqrt{L/(-\alpha)}=\xi_o[(T_{NA}-T)/T_{NA}]^{-1/2}$. The solution reads

$$\psi(z)=\frac{\psi_s}{\cosh\left(\dfrac{h}{\sqrt{2}\xi}\right)}\cosh\left(\frac{\sqrt{2}z}{\xi}\right). \tag{24}$$

Minimization of (21c) with respect to u gives

$$B\frac{\partial^2 u}{\partial z^2}=0 \tag{25a}$$

or

$$B\frac{\partial u}{\partial z}=B\frac{h-Nd}{Nd}=\sigma(h), \tag{25b}$$

where $\sigma(h)$ is the stress normal to the layer that can be calculated from the condition for mechanical equilibrium $\Delta p=\Pi_d=-\partial f/\partial h$ [Eq. (7)].

To do this calculation we must first determine the excess of free energy per unit surface. This gives after integration and by including van der Waals interactions

$$f(h)=\frac{-1}{\sqrt{2}}\alpha\xi\psi_s^2\left[th\left(\frac{h}{\sqrt{2}\xi}\right)-1\right]+\frac{\sigma(h)^2}{2B}h-\frac{A}{12\pi h^2} \tag{26}$$

from which we calculate

$$\Delta P=\Pi_d=+\frac{1}{2}\alpha\psi_s^2\left[1-th^2\left(\frac{h}{\sqrt{2}\xi}\right)\right]-\frac{\sigma^2}{2B}-\sigma-\frac{A}{6\pi h^3}. \tag{27}$$

Solving this equation gives the stress σ. It can be checked that to an excellent approximation the mechanical equilibrium is only set by the layer elasticity:

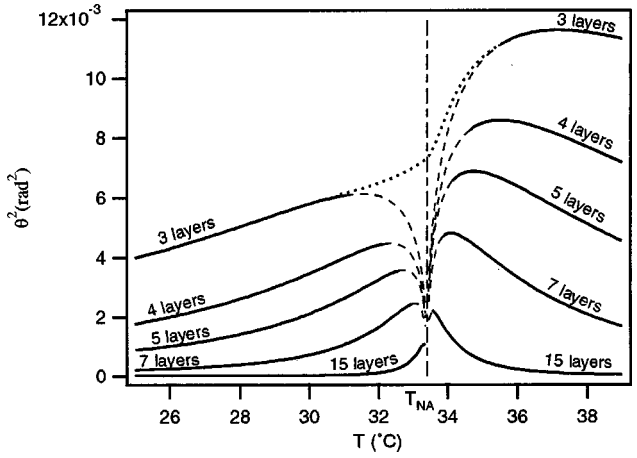

FIG. 6. Angle θ_m^2 as a function of temperature calculated for different values of the number of layers N from Eq. (26) at $T<T_{NA}$ and from Eqs. (32) and (10) at $T>T_{NA}$ by taking $\alpha_o\xi_o\psi_s^2/\gamma=7.4\times10^{-4}\,\mathrm{K}^{-1}$, $A=10k_BT$, and $\xi_o=0.8\,\mathrm{nm}$. The dashed parts of the theoretical curves have no physical meaning because the correlation length is larger than the film thickness. The dotted segment is just a hand-drawn extrapolation between high- and low-temperature parts of the theoretical curves.

$$\Delta P=-\sigma. \tag{28}$$

By contrast the associated elastic energy is very small (because B is very large) and completely negligible in our range of ΔP (see the discussion in the preceding section) in comparison to the other terms coming from the interaction between the free surfaces:

$$f(h)=\frac{-1}{\sqrt{2}}\alpha\xi\psi_s^2\left[th\left(\frac{h}{\sqrt{2}\xi}\right)-1\right]-\frac{A}{12\pi h^2}. \tag{29}$$

This formula also gives the contact angle θ_m and the film tension τ_N as a function of the number N of layers in the film:

$$\theta_m^2=\frac{-\alpha\xi\psi_s^2}{\sqrt{2}\gamma}\left[-th\left(\frac{Nd}{\sqrt{2}\xi}\right)\right]+\frac{A}{12\pi\gamma h^2}, \tag{30}$$

$$\tau_N=2\gamma+\Delta PNd+\frac{1}{\sqrt{2}}\alpha\xi\psi_s^2\left[1-th\left(\frac{Nd}{\sqrt{2}\xi}\right)\right]-\frac{A}{12\pi h^2}. \tag{31}$$

Equation (30) shows that θ_m does not depend on ΔP, in agreement with the experiment. In addition, this equation predicts the variation of θ_m^2 as a function of temperature, under the assumption that ψ_s is independent of the temperature (ψ_s should not have a critical behavior at T_{NA}). Theoretical curves $\theta_m^2(T)$ are displayed in Fig. 6 for different values of N by taking $\alpha_o\xi_o\psi_s^2/\gamma=7.4\times10^{-4}\,\mathrm{K}^{-1}$, $A=10k_BT$ and $\xi_o=0.8\,\mathrm{nm}$. These values have been chosen from a best fit of the experimental data (Figs. 3 and 4) far from the transition (solid parts of the theoretical curves), but the agreement is only qualitative. In particular, the prediction

that $\theta_m^2(T)$ passes through a maximum at a temperature $T_{\max}<T_{NA}$ and then goes to zero at T_{NA} is an artifact of the model. This is due to the fact that the correlation length ξ becomes larger than the film thickness above $T_{\max}$. In this limit, the finite size corrections play the most important role and the de Gennes model does not apply, so that the dashed parts of the theoretical curves close to T_{NA} are clearly wrong.

It turns out that the angle θ_m can be measured in overheated films at temperature $T>T_{NA}$. This problem is analyzed in the next section.

V. PRESMECTIC FILMS AND THINNING TRANSITIONS ABOVE T_{NA}

According to the de Gennes theory for presmectic films [6,7], there exists a temperature $T(N)$ above which a film with N layers spontaneously thins by one layer. $T(N)$ increases when N decreases, resulting in a succession of thinning transitions at increasing temperature. This phenomenon was first observed in fluorinated compounds [15] close to a first order smectic-*A*–isotropic phase transition, but the de Gennes theory is not directly applicable to this case [16]. It was then observed near the first order smectic-*A*–nematic phase transition of the liquid crystal 5O.6 [17] and near the second order smectic-*A*–nematic phase transition of liquid crystals 6O10 [18(a)] and 7AB [18(b)]. In the following, we show that thinning transitions are easily observable in 8CB too, where the phase transition is second order, provided the films are thick enough and the pressure difference is small. We then analyze our data in the framework of the Landau–de Gennes theory for the presmectic state. Finally, we calculate the contact angle θ_m above T_{NA}.

A. Thinning temperatures $T(N)$

The best way to observe thinning transitions in 8CB is to prepare thick films (100 layers typically) in contact with a meniscus of very large radius of curvature (2 mm or more). The pressure is measured by observing the meniscus profile and by using the Laplace law that still applies in the nematic phase. Once the film has been stretched, it is maintained at 33 °C (0.4 °C below T_{NA}) until all the dislocations have disappeared. Then, the temperature is raised by successive steps of 0.1 °C. After each temperature increment the film is observed under the microscope and its thickness is measured. Two cases can arise: either the film thickness does not change during 30 mn, which means that it will not change anymore, and we increase the temperature again; or elementary dislocation loops nucleate at the edge of the film (Fig. 7). These loops wet the meniscus, grow and merge together resulting in a film thickness variation by one layer. In this case, we wait typically 3 hours at the same temperature in order that the film and its meniscus are again stabilized. The temperature is then again increased by 0.1 °C and so on. In this way, it was possible to measure the temperature $T(N)$ as a function of the number of layers N (circles in Fig. 8). We also performed a similar experiment by imposing a larger increment of temperature (triangles in Fig. 8). In this case, the film thins by more than one layer after each increment.

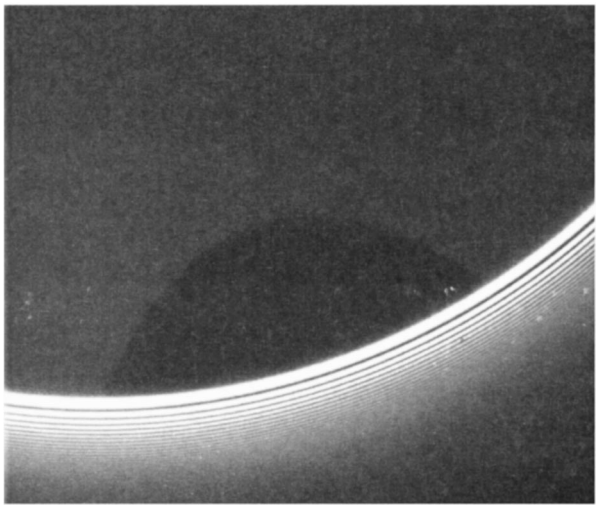

FIG. 7. Loop of dislocation nucleating at $T(N)$ on the side of the meniscus.

On the other hand, the two curves are superimposed, which means that the final number of layers (which is also the number of layers above which the film is unstable) is a universal function of the temperature. Note that ΔP was almost the same (65 and 70 dyn/cm^2) in these two experiments, which is important for comparing the results even if the curve $T(N)$ as a function of N does not depend strongly on ΔP. Indeed, we found that $T(N)$ slightly decreases (by about 0.2 K) when the pressure difference equals $\Delta P=400$ dyn/cm^2. Note also that we have no data for films thinner than 10 layers because above 40.4 °C the films break because of the nucleation of small droplets of isotropic liquid (this temperature coincides with the nematic–isotropic transition temperature).

B. Landau–de Gennes theory of the presmectic state

The same theory may be used to calculate temperatures $T(N)$. The phase of the order parameter (which is related to

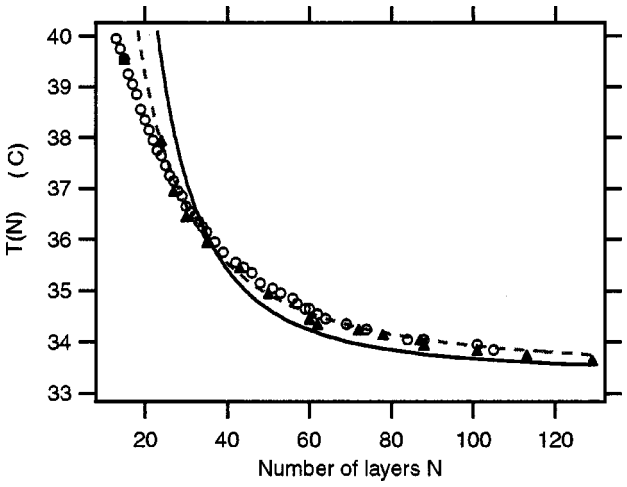

FIG. 8. Thinning temperature $T(N)$ as a function of N. Circles: $\Delta P=65$ dyn/cm^2; triangles $\Delta P=70$ dyn/cm^2. The solid line has been calculated from the model [Eq. (37)] by taking $\Delta P=70$ dyn/cm^2. The dashed line is the best fit to a power law $[T(N)=T_{NA}(1+aN^{-1/\nu})]$ with $\nu=0.69\pm0.05$ and $a=13$.

the layer displacement u) must again be taken into account in the calculations because the film is much ''softer'' above T_{NA} than below, so that the compression energy (14) becomes more important.

A straightforward calculation, including the phase $\phi = 2\pi u/d$ of the order parameter (note that as $\Psi_b = 0$ above T_{NA}, $\Psi = \psi$), gives with our notations [19]

$$f(h) = \alpha \xi \psi_s^2 \left[\tanh\left(\frac{h}{2\xi}\right) + \frac{1-\cos[\phi]_N}{\sinh(h/\xi)} - 1 \right]. \tag{32}$$

We define the correlation length above T_{NA} as

$$\xi = \sqrt{\frac{L}{\alpha}} \quad \text{with} \quad \alpha = \alpha_o (T - T_{NA}) \tag{33}$$

and we set

$$[\phi]_N = \frac{2\pi}{d}(h - Nd), \tag{34}$$

where h is the actual thickness of the film. As noted in Ref. [7], there are forbidden gaps, where the compressibility is negative ($\partial^2 f/\partial h^2 < 0$) which correspond to absolutely unstable ''presmectic'' states, and stable (or more exactly, metastable) bands, where $\partial^2 f/\partial h^2 > 0$. From the last condition, it follows that for admissible bands one has (by assuming that $h \gg \xi \gg d/2\pi$):

$$|h - Nd| \leqslant \frac{d}{4}. \tag{35}$$

In this case, the equation for mechanical equilibrium (7) becomes

$$\Delta P = -\frac{4\pi}{d} \alpha \xi \psi_s^2 \exp\left(\frac{-Nd}{\xi}\right) \sin[\phi]_N. \tag{36}$$

In practice ΔP is fixed by the meniscus and condition (36) gives all the admissible solutions at a given temperature (Fig. 9). In particular, we see that for each ΔP, there exists a critical thickness H_c above which all films of thickness $H > H_c$ are absolutely unstable. The critical thickness H_c decreases as the temperature increases because the amplitude of the disjoining pressure decreases when the temperature increases. In practice we measure the temperature $T(N)$ at which $H_c = Nd$. It is given by simply setting $\sin[\phi]_N = -1$ in Eq. (36). This gives an equation for $T(N)$ of the form

$$\Delta P = \frac{4\pi}{d} \alpha[T(N)] \xi[T(N)] \psi_s^2 \exp\left(\frac{-Nd}{\xi[T(N)]}\right) \tag{37}$$

or, by including van der Waals interactions

$$\Delta P = \frac{4\pi}{d} \alpha[T(N)] \xi[T(N)] \psi_s^2 \exp\left(\frac{-Nd}{\xi[T(N)]}\right) + \frac{A}{6\pi N^3 d^3}. \tag{38}$$

This equation allows us to calculate numerically $T(N) - T_{NA}$ by using our previous estimate of $\alpha_o \xi_o \psi_s^2/\gamma$, A, and ξ_o. It gives the solid line in Fig. 8. The agreement with the experimental points is qualitatively correct. Note that, with typical values for A, van der Waals interactions are so small that (37) and (38) give almost the same result.

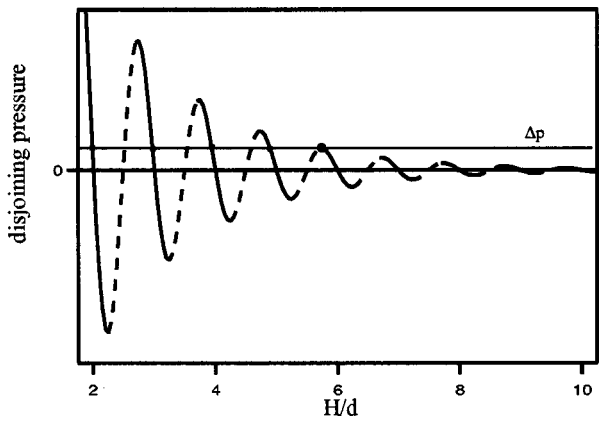

FIG. 9. Theoretical disjoining pressure as a function of N. The thick segments represent the allowed bands whereas dashed ones represent thermodynamically unstable states. The horizontal line represents the pressure ΔP that is imposed by the meniscus. The points of intersection with the thick segments of the curve determine the spectrum of all the possible metastable solutions (superheated films).

To say more would require further knowledge of the specific mechanisms that lead to layer thinning transitions. These mechanisms should obviously take into account dynamic and kinetic processes (including, e.g., nucleation of elementary dislocation loops). All these phenomena are beyond the scope of our paper. Let us note only that for the dislocation mechanism of layer thinning transitions, the activation energy is well known (see, e.g., Refs. [4,5,16]) and reads for a homogeneous nucleation process:

$$E_{\text{act}} = \frac{\pi E^2}{d\Delta P}, \tag{39}$$

where E is the line tension of an elementary edge dislocation including ''bulk'' elastic deformation energy E_b as well as a surface contribution E_s. In the framework of the usual elasticity, both contributions can be calculated. The former reads [20]

$$E_b \approx \sqrt{KB}\frac{d^2}{\xi} \tag{40}$$

by taking ξ as an estimation for the core radius, while the latter has been calculated in Ref. [21] and equals

$$E_s \approx \sqrt{\gamma B d}\frac{d}{H}. \tag{41}$$

For the natural values of the parameters, E_{act} is of the order of $10 k_B T$ only very close to the temperatures $T(N)$ found from Eqs. (34) and the fact that the nucleation is heterogeneous (loops nucleate on the side of the meniscus) should not change this conclusion. Out of this region $E_{\text{act}} \gg 10 k_B T$ and

therefore the probability for nucleating of an elementary dislocation loop (even in the central part of the film where B is minimal) is completely negligible.

C. Contact angle θ_m above T_{NA}

The contact angle θ_m between an overheated film and its meniscus can be obtained by first solving Eq. (36) in $[\phi]_N$. The parameters chosen are the same as before: $\alpha_o \xi_o \psi_s^2/\gamma = 7.4\times 10^{-4}\,\mathrm{K}^{-1}$, $A = 10 k_B T$, $\xi_o = 0{,}8\,\mathrm{nm}$ with $\Delta P = 250\,\mathrm{dyn/cm}^2$ which is a typical value in our experiments. Knowing $[\phi]_N$ (note that $\cos[\phi]_N \approx 1$ when $T - T_{NA}$ is larger than 0.1 °C) we then calculate $f(h)$ and θ_m^2 using Eq. (32) and Eq. (10). The theoretical curves $\theta_m^2(T)$ are displayed in Fig. 6 for different values of N. As before, each curve contains a part that has no physical meaning because the correlation length is larger than the film thickness (dashed parts of the curves, on the left of the maxima). On the other hand, these curves predict that the contact angle is larger above T_{NA} than below, passes through a maximum, and decreases at high temperature. These results are again in good qualitative agreement with experiments (see Fig. 4).

VI. CONCLUDING REMARKS

In fact, the question of layer thinning transitions is from a thermodynamical point of view equivalent to the question of the dependence of the smectic-A–nematic transition temperature $T(N)$ on the film thickness (or on N).

There are two effects related to the existence of the surface. The first is purely geometrical. Indeed, surfaces break translational and orientational invariances (the surface is a specific plane that breaks the translational invariance while the normal to the surface defines a specific direction that violates the rotational invariance). These geometrical effects lead to the finite size screening of fluctuations and are the sources for the pseudo-van der Waals interactions mentioned above. In addition, when the correlation length increases and becomes larger than the thickness of the film, the system can be considered as homogeneous (nonfluctuating) in the z direction, so that a global large-scale description in this regime would be closer to two-dimensional (2D) model instead of a three-dimensional (3D) model. Therefore a 3D–2D crossover should take place at temperatures that scale as

$$\frac{\xi}{Nd} \approx 1. \tag{42}$$

This relation defines a temperature interval $[T_{NA} - \delta T_{co}, T_{NA} + \delta T_{co}]$ around T_{NA} in which the previous theory does not apply (dotted segment in Fig. 6). The crossover temperature range δT_{co} scales as a function of N like

$$\frac{\delta T_{co}}{T_{NA}} \alpha N^{-1/\nu}, \tag{43}$$

where ν is the exponent for the bulk correlation length. In the mean field approximation $\nu = 1/2$, and therefore $\delta T_{co} \alpha N^{-2}$.

The second effect of the surfaces is related to the physical modifications of the system at the surfaces due to, e.g., missing neighbors, or to the interactions with the environment and so on. In the preceding section we have assumed that this effect was responsible for an increase of the smectic order parameter at the free surfaces and that $\Psi = \Psi_s$ at the two surfaces irrespective of the temperature. But we can set other boundary conditions at the free surfaces. For example, we can consider, as de Gennes did in Ref. [6], that Ψ is not constant at the free surfaces, but rather is given by minimizing some surface free energy of the form

$$f_s = -h_s[\Psi(h/2) + \Psi(-h/2)]. \tag{44}$$

This expression fixes the order parameter gradient rather than its value at the free surfaces. Similar calculations [6] in the limit $h \gg \xi \gg d/2\pi$ shows that temperatures $T(N)$ verify

$$\Delta P = \frac{4\pi}{d} \frac{h_s^2}{\alpha[T(N)]\xi[T(N)]} \exp\left(\frac{-Nd}{\xi[T(N)]}\right). \tag{45}$$

This result is similar as before and Eqs. (45) and (37) give the same scaling for $T(N)$:

$$\frac{Nd}{\xi[T(N)]} = C, \tag{46}$$

where C is approximately constant within a logarithmic correction in Δp and $T(N) - T_{NA}$. We emphasize that $C \gg 1$ and therefore the assumption $h \gg \xi$ is valid at $T(N)$. Equation (46) can also be rewritten in the form $([T(N) - T_{NA}]/T_{NA})\alpha(1/N^2)$. This law is not very well verified experimentally. A reasonable assumption would be to assume that Eq. (46) is general and applies to other models. In this case,

$$\frac{T(N) - T_{NA}}{T_{NA}} \alpha \frac{1}{N^{1/\nu}}, \tag{47}$$

where ν is the critical exponent for the correlation length ($\xi = \xi_o[(T - T_{NA})/T_{NA}]^{-\nu}$). The best fit of the experimental values (Fig. 8) gives $\nu = 0.69 \pm 0.05$. This value is in agreement with that found in x-ray experiments ($\nu = 0.67 \pm 0.03$ [22(a)] and $\nu = 0.70 \pm 0.03$ [22(b)]) or light scattering experiments ($\nu = 0.72 \pm 0.05$ [22(b)]) and coincides with the theoretical value $\nu = 0.67$ given by the XY model. We note however in Fig. 8 that the fit of $T(N)$ to a power law is very good below 38 °C, but deviates at larger temperatures when the nematic-to-isotropic phase transition temperature is approached (we measured $T_{IN} = 40.4\,°\mathrm{C}$). This observation is perhaps the signature of some pretransitional effects close to the N–I phase transition.

ACKNOWLEDGMENTS

We are grateful to J.C. Géminard and P. Pieranski for fruitful discussions and suggestions. This work was supported by the European Research Network Contract No. FMRX-CT0085. E.K. acknowledges with appreciation the support from the Ecole Normale Supérieure de Lyon.

[1] G. Friedel, Ann. Phys. (Paris) **18**, 273 (1922).
[2] P. S. Pershan, *Structure of Liquid Crystal Phases* (World Scientific, Singapore, 1988).
[3] P. Pieranski *et al.*, Physica A **194**, 364 (1993).
[4] J. C. Géminard, R. Holyst, and P. Oswald, Phys. Rev. Lett. **78**, 1924 (1997).
[5] F. Picano, R. Holyst, and P. Oswald, Phys. Rev. E **62**, 3747 (2000).
[6] P. G. de Gennes, Langmuir **6**, 1448 (1990).
[7] E. E. Gorodetskiĭ, E. S. Pikina, and V. E. Podnek, JETP **88**, 35 (1999).
[8] A. Yethiraj and J. Bechhoefer, ''Using nematic director fluctuations as a sensitive probe of the nematic–smectic-A phase transition in liquid crystals,'' Conference Proceedings for ''International Liquid Crystal Conference 16,'' Kent, OH, June 24–28, 1996; Mol. Cryst. Liq. Cryst. **304**, 301 (1997).
[9] For a recent review, see V. Bergeron, J. Phys.: Condens. Matter **11**, R215 (1999).
[10] M. Benzekri, T. Claverie, J. P. Marcerou, and J. C. Rouillon, Phys. Rev. Lett. **68**, 2480 (1992).
[11] J. Israelachvili, *Intermolecular & Surface Forces*, 2nd ed. (Academic, London, 1992).
[12] A. Ajdari, L. Peliti, and J. Prost, Phys. Rev. Lett. **66**, 1481 (1991).
[13] P. Richetti, P. Kékicheff, and P. Barois, J. Phys. II **5**, 1129 (1995).
[14] P. G. de Gennes and J. Prost, *The Physics of Liquid Crystals* (Oxford University Press, Oxford, England, 1995).
[15] T. Stoebe, P. Mach, and C. C. Huang, Phys. Rev. Lett. **73**, 1384 (1994); P. M. Johnson, P. Mach, E. D. Wedell, F. Lintgen, M. Neubert, and C. C. Huang, Phys. Rev. E **55**, 4386 (1997); S. Pankratz, P. M. Johnson, H. T. Nguyen, and C. C. Huang, *ibid.* **58**, R2721 (1998).
[16] S. Pankratz, P. M. Johnson, R. Holyst, and C. C. Huang, Phys. Rev. E **60**, R2456 (1999).
[17] E. I. Demikhov, V. K. Dolganov, and K. P. Meletov, Phys. Rev. E **52**, R1285 (1995).
[18] (a) V. K. Dolganov, E. I. Demikhov, R. Fouret, and C. Gors, Phys. Lett. A **220**, 242 (1996); (b) E. A. L. Mol, G. C. L. Wong, J. M. Petit, F. Rieutord, and W. H. de Jeu, Physica B **248**, 191 (1998).
[19] L. Moreau, P. Richetti, and P. Barois, Phys. Rev. Lett. **73**, 3556 (1994); P. Richetti, L. Moreau, P. Barois, and P. Kékicheff, Phys. Rev. E **54**, 1749 (1996).
[20] M. Kléman and C. E. Williams, J. Phys. (France) Lett. **35**, L49 (1974).
[21] L. Lejcek and P. Oswald, J. Phys. II **1**, 931 (1991); R. Holyst and P. Oswald, Int. J. Mod. Phys. B **9**, 1515 (1995).
[22] (a) D. Davidov, C. R. Safinya, M. Kaplan, S. S. Dana, R. Schaetzing, R. J. Birgeneau, and J. D. Lister, Phys. Rev. Lett. **31**, 1657 (1979); (b) S. Sprunt, L. Solomon, and J. D. Litser, *ibid.* **53**, 1923 (1984).